SINGLE-SHOT FRACTIONAL FOURIER PHASE RETRIEVAL

Yixiao Yang and Ran Tao

School of Information and Electronics, Beijing Institute of Technology, Beijing, China

ABSTRACT

Traditional phase retrieval is generally concerned with recovering a signal from its Fourier magnitude measurements whose inherent ambiguities make this problem especially difficult. In this work, we present an efficient phase retrieval technique from the single fractional Fourier transform (FrFT) magnitude measurement. Specifically, the FrFT measurement can be well-combined with signal priors via a generalized alternating projection framework, which can effectively alleviate the ambiguities of phase retrieval and the stagnation problem of numerical iterative processes. Through numerical simulations, we demonstrate that reconstructing an image from the single FrFT measurement leads to a significant performance improvement over that from the Fourier transform magnitude by using the proposed method. The source code is available at https://github.com/Yixiao-Yang/SFrFPR.

Index Terms— Phase retrieval, fractional Fourier transform, single-shot, generalized alternating projection

1. INTRODUCTION

Phase Retrieval (PR) is a long-established challenge for estimating a signal from the phase-less linear measurements, encountered in various engineering fields including x-ray crystallography [1], microscopy [2], holography [3], and computational imaging [4]. In optical detection systems, the measurable quantity is the photon flux, which is proportional to the magnitude-square of a light wave. Furthermore, the observation in the far-field of diffraction or the focal plane of a lens can be formulated by the Fourier transform, which provides the possibility of Fourier PR [5].

Nevertheless, the Fourier PR problem is not uniquely solvable without extra prior information due to the lack of phase [6]. There exist trivial ambiguities caused by translation and inversion of the target and non-trivial ambiguities, which conserve the Fourier magnitude measurement [7]. As a result, standard PR algorithms suffer from serious stagnation and produce inaccurate solutions [8]. Therefore, it is of paramount importance to employ additional knowledge to reduce the set of ambiguities or even to ensure uniqueness.
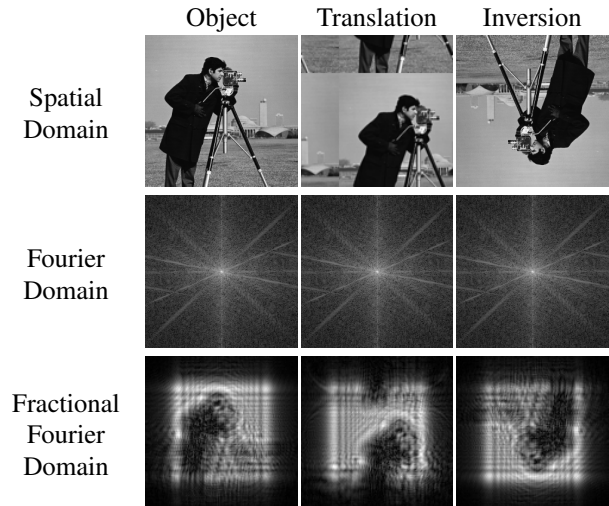
Fig. 1. Operation of translation or inversion on the object corresponds to the same magnitude in the Fourier domain, but a different one in the Fractional Fourier domain. Here we adopt the 0.5th-order fractional Fourier transform.

Over the years, several physical observation systems have been developed, which record redundant measurements to mitigate the ambiguities and algorithmic issues of PR. A popular example is coherent diffraction imaging (CDI), which recovers an underlying object from the oversampled coherent diffraction patterns in the far-field, given known image support [9]. In terms of signal processing, this problem corresponds to reconstructing a two-dimensional signal from its oversampled Fourier transform magnitude [10]. The trivial ambiguity caused by signal shift can be avoided with compact support. A further idea to obtain additional observations is coded diffraction patterns (CDP), which use several exposures with different masks to produce multiple diffraction measurements [11]. This technique is based on the principle that different masks can modulate the signal of interest and introduce information redundancy to reduce ambiguities [12]. Another method to increase observation diversity is scanning CDI or ptychography, which adopts the adjacent illumination patterns to acquire a set of measurements [13]. The main idea is to estimate a signal from measurements of short-time Fourier transform magnitude with an overlapped window between adjacent short-time sections [14]. Nevertheless, those observation systems introduce extra physical devices and

measurement models involving high computational complexity, which bring a burden to practical applications [15, 16].

In fact, the above optical settings assume that measurements are taken at the Fourier plane or Fraunhofer regime. However, the intensity pattern can be collected at an arbitrary plane between the object field and the far-field, which would imply the new measurement model that is different from Fourier transform [5]. In this context, the most prominent case is the regime of Fresnel diffraction, where the propagation-evolution of electromagnetic waves at an arbitrary distance away from the object plane can be described as an integral form, termed Fresnel integral [17]. Moreover, fractional Fourier transform (FrFT) as a well-defined signal processing tool can be introduced here, which is a generalization of the Fourier transform [18, 19]. This is due to an equivalent relation between FrFT and Fresnel integral, just like the Fourier transform and Fraunhofer integral [20]. The advantages to be gained from this connection are obvious: FrFT provides a new signal processing perspective into describing the propagation of light, not limited to the spatial or Fourier domains. In addition, compared with the Fresnel integral, good theoretical properties and fast numerical algorithms of FrFT can benefit the practical usage. Thus, this gives rise to a few works on the problem of phase retrieval from multiple FrFT magnitude measurements [21, 22]. However, they still require a lot of observations to ensure recovery and ignore algorithmic improvements.

Towards this dilemma, we first address the problem of reconstructing a two-dimensional image from the single FrFT magnitude measurement, called Single-shot Fractional Fourier Phase Retrieval (SFrFPR). To this end, we employ the generalized alternating projection scheme to ensure the measurement fidelity and statistical prior regularization. A key idea is that the single FrFT measurement combined with some simple image priors (e.g., real-valued) can effectively mitigate ambiguities of PR, relaxing the previous conditions on oversampled or multiple measurements. In contrast to the Fourier measurement, SFrFPR can largely alleviate the stagnation problem of the reconstruction algorithms. Numerical simulations validate the superiority of the proposed SFrFPR.

2. METHOD

In this section, we recall the relationship between FrFT and Fresnel integral, and formulate the FrFT-based measurement model. Then we adopt the generalized alternating projection (AP) algorithm to solve this problem. Compared with Fourier PR, we analyze the properties and advantages of SFrFPR.

2.1. Measurement Model based on FrFT

Based on Maxwell's equations and reasonable simplifications, the propagation of light on two planar surfaces along the axis z can be characterized by Fresnel integral [23]:

$$U_z(u,v) = \frac{e^{i\frac{2\pi}{\lambda}z}}{i\lambda z} \iint_{-\infty}^{\infty} U_0(x,y)e^{i\frac{\pi}{\lambda z}[(u-x)^2+(v-y)^2]}dxdy,$$
(1)

where λ is the wavelength of light.

The two-dimensional FrFT of the optical field $U_0(x,y)$ is defined as

$$\mathcal{F}_\alpha[U_0](u,v) = \iint_{-\infty}^{\infty} K_\alpha(u,x)K_\alpha(v,y)U_0(x,y)dxdy,$$
(2)

where $K_\alpha(u,x) = \sqrt{1-i\cot\alpha}e^{i\pi(\cot\alpha u^2 - 2\csc\alpha ux + \cot\alpha x^2)}$ denotes the kernel function with $\alpha = \frac{\pi}{2}p$ [18]. Here p is the fractional order with $0 < |p| < 2$. Specially, the FrFT reduces to the (inverse) Fourier transform when $p = \pm1$.

To connect the Fresnel integral (1) and FrFT (2), we introduce the scaled fields $\hat{U}_z(u,v) \equiv U_z(s_2u,s_2v), \hat{U}_0(x,y) \equiv U_0(s_1x,s_1y)$ with $s_1 = \sqrt{\frac{\lambda z}{\tan\alpha}}, s_2 = \sqrt{\frac{\lambda z}{\sin\alpha\cos\alpha}}$ and obtain

$$\hat{U}_z(u,v) = \frac{e^{i\frac{2\pi}{\lambda}z}}{i\tan\alpha+1}e^{i\pi\tan\alpha(u^2+v^2)}\mathcal{F}_\alpha[\hat{U}_0](u,v),$$
(3)

Considering the amplitude-only measurement, the spherical phase factor of (3) disappears and we can have

$$|\hat{U}_z(u,v)| = \frac{1}{\sqrt{\tan^2\alpha+1}}|\mathcal{F}_\alpha[\hat{U}_0](u,v)|,$$
(4)

Thereby, we conclude that the scaled amplitude distribution of light at an intermediate plane can be interpreted as the FrFT magnitude. In practice, given the scale factor s_1 and the propagation distance z, we can know exactly the other scale factor $s_2 = s_1\sqrt{1+\frac{(\lambda z)^2}{s_1^4}}$ and the corresponding fractional order $p = \frac{2}{\pi}\arctan(\frac{\lambda z}{s_1^2})$. In the scope of this work, we only focus on the FrFT magnitude measurement.

2.2. Generalized AP Algorithm

Now the SFrFPR problem can be mathematically stated as

$$Given \quad y = |\mathcal{F}_\alpha x|, \qquad find \quad x. \quad (5)$$

Suppose M and S are two constraint sets in $\mathbb{C}^{n\times n}$ that ensure measurement consistency and signal prior, respectively. Given a feasible initial point x_0, the generalized AP framework alternately [24] projects onto M and S:

$$v_k = P_M(x_{k-1}), x_k = P_S(v_k), k = 1,2,3,..., \quad (6)$$

where P_M and P_S denote projection on M and S.

The typical operation of P_M is enforcing the measurement-fidelity constraint, i.e.,

$$P_M(x_k) = \mathcal{F}_{-\alpha}\left(y \circ \frac{\mathcal{F}_\alpha x_k}{|\mathcal{F}_\alpha x_k|}\right),$$
(7)

where ∘ denotes the Hadamard (element-wise) product and $\mathcal{F}_{-\alpha}$ denotes the inverse transformation of $\mathcal{F}_{\alpha}$.

For the implementation of P_S, the most commonly used priors are real-valued, smoothness, and sparsity. Inspired by the recent deep plug-and-play (PnP) technique [25], the inherent image priors can be implicitly imposed via solving a regularized denoising problem:

$$P_S(v_k) = \arg\min_x \left\{ \mathcal{R}(x) + \frac{1}{2\sigma^2}\|x - v_k\|_2^2 \right\}, \qquad (8)$$

where $\mathcal{R}(x)$ denotes a prior regularization term and σ is a parameter about noise level.

And this problem can be solved by using any off-the-shelf denoiser $\mathcal{H}_\sigma$, i.e., $P_S(v_k) = \mathcal{H}_\sigma(v_k)$. In this way, the resulting iterations follow (6), (7) and (8).

2.3. FrFT vs Fourier Measurement

Next we present the FrFT measurement has many unique and useful properties that make it attractive. Specifically, the FrFT measurement has the space-frequency coupling characteristics [18], which holds features of signals both on spatial domain and frequency domain. Therefore, some changes of signal on spatial domain also have effects on the FrFT measurement. For example, signals of space-shift and conjugate-inversion will produce the different FrFT measurements according to the spatial shift and reversal property of the FrFT [26], respectively, shown in Fig. 1.

Moreover, the FrFT measurement constraint can be well combined with spatial characteristics of images such as real-valued or other inherent priors to further reduce ambiguities, illustrated in Fig. 2. On the contrary, the Fourier measurement constraint will not work with image priors (e.g., real-valued), suffering from the stagnation problem of numerical iterative processes. The reason can be found in Remark 1 and Remark 2. As a result, these properties of FrFT measurement play a big role in alleviating the ambiguities of PR and stagnation problem of reconstruction algorithm, enabling it to stand out.

Remark 1 *Suppose the ground-truth $x \in \mathbb{R}^{n \times n}$ and the initial point $x_0 \in \mathbb{R}^{n \times n}$, we consider $P_S(v_k) = real(v_k)$ and $P_M(x_k) = \mathcal{F}^{-1}\left(|\mathcal{F}x| \circ \frac{\mathcal{F}x_k}{|\mathcal{F}x_k|}\right)$ where $real(\cdot)$ denotes the operation of taking the real part and $\mathcal{F}$ is the Fourier transform. Then we can have $x_k = P_S(P_M(x_{k-1})) = P_M(x_0), k = 1, 2, 3, ...$, which can be derived by the properties of Fourier spectrum of real signals.*

Remark 2 *Under same conditions as in Remark 1 except $P_M(x_k) = \mathcal{F}_{-\alpha}\left(|\mathcal{F}_\alpha x| \circ \frac{\mathcal{F}_\alpha x_k}{|\mathcal{F}_\alpha x_k|}\right)$ with $\alpha \neq \pm\frac{\pi}{2}$, we can obtain that x_k will converge to a fixed point x^*, which can be validated by numerical simulations, shown in Fig. 4.*
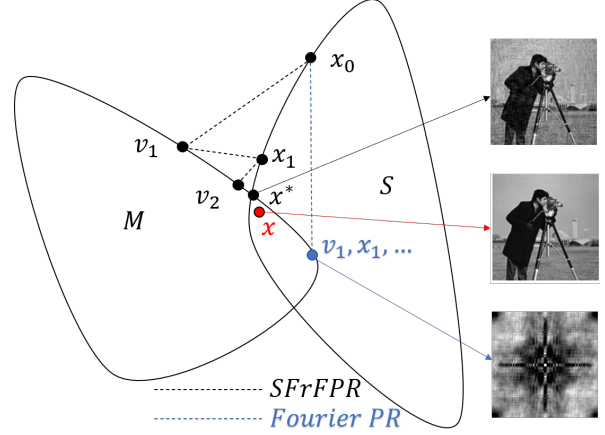

Fig. 2. The illustration of numerical iterative processes of generalized AP algorithm. Here M is the FrFT or Fourier measurement-fidelity set and S is the set of real signals.

3. NUMERICAL SIMULATIONS

In this section, numerical simulations evaluate the proposed method. First, we present the simulation setup. Then we compare the performance of FrFT measurements with different fractional orders using several PR algorithms. Finally, we further investigate the effectiveness of FrFT measurement.

3.1. Simulation Setup

In this paper, we use the eigen decomposition-type discrete FrFT [27]. We adopt six PR methods, including classic approach Wirtinger Flow (WF) [12] with real-valued prior and generalized alternating projection (GAP) approaches with various image priors such as real-valued, total variation (tv) [28], weighted nuclear norm minimization (wnnm) [29], block-matching and 3d filtering (bm3d) [30], and denoising convolutional neural network (dncnn) [31]. We create our own version of WF based on the original code, revised for the FrFT measurement. For the denoisers involved, we use the code made available by the respective authors' websites. In addition, we adopt a public dataset Set12 to quantitatively evaluate the algorithmic performance, which includes twelve widely-used testing images. For simplicity, all images are resized to 128×128. The iteration number empirically sets to 200 and we adopt all-one initialization for performance comparison.

Table 1. The average PSNRs (dB) of 128×128 reconstructions from FrFT measurements with different orders using six PR algorithms across the testing set.

	$p = 0.1$	$p = 0.3$	$p = 0.5$	$p = 0.7$	$p = 1$
WF-real	33.46	30.82	28.90	26.10	11.14
GAP-real	34.77	32.05	29.99	26.94	11.14
GAP-tv	32.25	32.40	32.96	33.13	11.23
GAP-wnnm	33.78	33.82	34.08	33.93	11.18
GAP-bm3d	34.95	35.17	35.57	35.46	11.14
GAP-dncnn	39.82	38.11	40.31	34.77	11.14

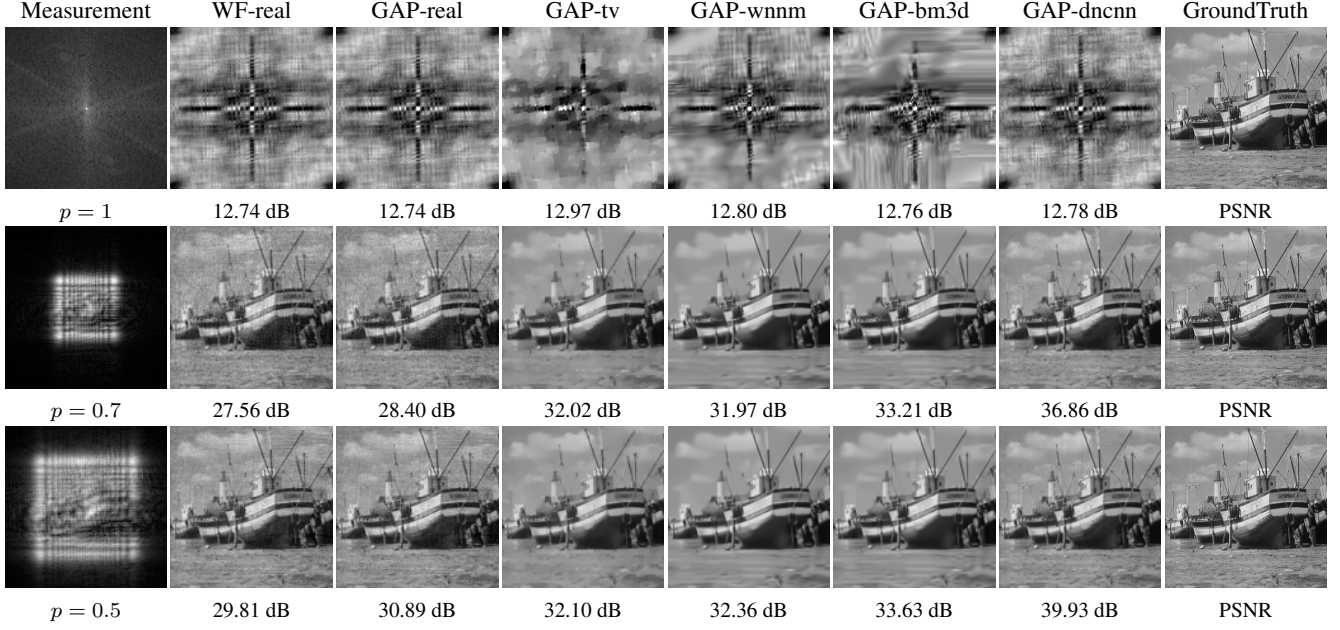| Measurement	WF-real	GAP-real	GAP-tv	GAP-wnnm	GAP-bm3d	GAP-dncnn	GroundTruth
$p=1$	12.74 dB	12.74 dB	12.97 dB	12.80 dB	12.76 dB	12.78 dB	PSNR
$p=0.7$	27.56 dB	28.40 dB	32.02 dB	31.97 dB	33.21 dB	36.86 dB	PSNR
$p=0.5$	29.81 dB	30.89 dB	32.10 dB	32.36 dB	33.63 dB	39.93 dB	PSNR

Fig. 3. Reconstruction results (PSNR) of six PR methods on FrFT measurements with different orders ($p=1$, $p=0.7$, and $p=0.5$, from top to bottom).

3.2. Performance Comparison

In this subsection, we compare the performance of FrFT measurements with different fractional orders using six PR algorithms. Table 1 reports the average recovery accuracy in terms of mean peak-signal-to-noise ratio (PSNR) on testing dataset Set12. It can be observed that all PR methods consistently perform well on FrFT measurements with different fractional orders except $p=1$ that denotes the Fourier transform measurement. Moreover, the reconstructing performance can be dramatically improved with the advanced denoisers when using the FrFT measurement. On the contrary, all PR algorithms suffer from serious stagnation and fail to recover images from the Fourier transform measurement. Fig. 3 visually shows the reconstructions of all PR algorithms from FrFT measurements with three fractional orders, i.e., $p=1, 0.7, 0.5$, respectively. It can be seen that all PR algorithms can reconstruct satisfactory images from the single FrFT measurement but fail from the Fourier transform measurement.

3.3. Discussion

To further investigate the effectiveness of the proposed method, we show the convergence behaviors of the FrFT measurements with different orders using the GAP-real algorithm. Fig. 4 presents the norm distance between the reconstructed signal and the ground-truth varies with iterations. It can be found that the error distance can gradually get smaller and converge to a fixed point from the single FrFT measurement. However, the GAP-real algorithm suffers from serious stagnation and produces an inaccurate solution from the Fourier transform measurement. Therefore, we empirically validate
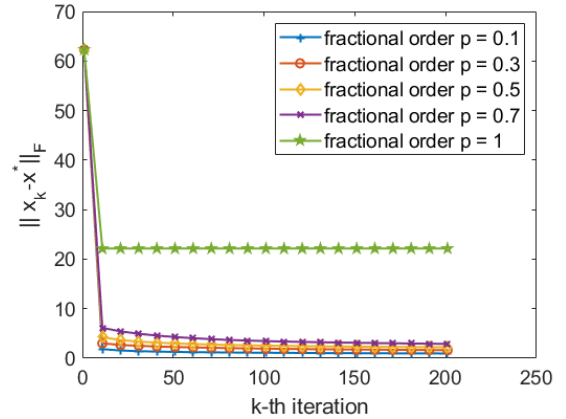

Fig. 4. Convergence behaviors of the FrFT measurements with different orders using the GAP-real algorithm.

that the FrFT measurement can be well-combined with image priors to effectively avoid the stagnation problem.

4. CONCLUSION

In this work, we are the first to address the problem of phase retrieval from the single FrFT measurement. To this end, we adopt the generalized alternating projection scheme that combines properties of the FrFT measurement with image priors, relaxing the previous conditions of oversampled or multiple measurements. Through numerical simulations, we demonstrate that the single FrFT measurement dramatically outperforms the Fourier transform measurement using several PR algorithms. We believe the proposed SFrFPR can provide new possibilities in near-field quantitative phase imaging.

5. REFERENCES

[1] Jianwei Miao, David Sayre, and HN Chapman, "Phase retrieval from the magnitude of the fourier transforms of nonperiodic objects," *JOSA A*, vol. 15, no. 6, pp. 1662–1669, 1998.

[2] Guoan Zheng, Roarke Horstmeyer, and Changhuei Yang, "Wide-field, high-resolution fourier ptychographic microscopy," *Nature photonics*, vol. 7, no. 9, pp. 739–745, 2013.

[3] Praneeth Chakravarthula, Ethan Tseng, Tarun Srivastava, Henry Fuchs, and Felix Heide, "Learned hardware-in-the-loop phase retrieval for holographic near-eye displays," *ACM Transactions on Graphics (TOG)*, vol. 39, no. 6, pp. 1–18, 2020.

[4] Ori Katz, Pierre Heidmann, Mathias Fink, and Sylvain Gigan, "Non-invasive single-shot imaging through scattering layers and around corners via speckle correlations," *Nature photonics*, vol. 8, no. 10, pp. 784–790, 2014.

[5] Yoav Shechtman, Yonina C Eldar, Oren Cohen, Henry Nicholas Chapman, Jianwei Miao, and Mordechai Segev, "Phase retrieval with application to optical imaging: a contemporary overview," *IEEE signal processing magazine*, vol. 32, no. 3, pp. 87–109, 2015.

[6] L Taylor, "The phase retrieval problem," *IEEE Transactions on Antennas and Propagation*, vol. 29, no. 2, pp. 386–391, 1981.

[7] MHMH Hayes, "The reconstruction of a multidimensional sequence from the phase or magnitude of its fourier transform," *IEEE Transactions on Acoustics, Speech, and Signal Processing*, vol. 30, no. 2, pp. 140–154, 1982.

[8] JR Fienup and CC Wackerman, "Phase-retrieval stagnation problems and solutions," *JOSA A*, vol. 3, no. 11, pp. 1897–1907, 1986.

[9] Jianwei Miao, Tetsuya Ishikawa, Ian K Robinson, and Margaret M Murnane, "Beyond crystallography: Diffractive imaging using coherent x-ray light sources," *Science*, vol. 348, no. 6234, pp. 530–535, 2015.

[10] James R Fienup, "Reconstruction of an object from the modulus of its fourier transform," *Optics letters*, vol. 3, no. 1, pp. 27–29, 1978.

[11] Emmanuel J Candes, Xiaodong Li, and Mahdi Soltanolkotabi, "Phase retrieval from coded diffraction patterns," *Applied and Computational Harmonic Analysis*, vol. 39, no. 2, pp. 277–299, 2015.

[12] Emmanuel J Candes, Xiaodong Li, and Mahdi Soltanolkotabi, "Phase retrieval via wirtinger flow: Theory and algorithms," *IEEE Transactions on Information Theory*, vol. 61, no. 4, pp. 1985–2007, 2015.

[13] Franz Pfeiffer, "X-ray ptychography," *Nature Photonics*, vol. 12, no. 1, pp. 9–17, 2018.

[14] Kishore Jaganathan, Yonina C Eldar, and Babak Hassibi, "Stft phase retrieval: Uniqueness guarantees and recovery algorithms," *IEEE Journal of selected topics in signal processing*, vol. 10, no. 4, pp. 770–781, 2016.

[15] Lei Tian, Ziji Liu, Li-Hao Yeh, Michael Chen, Jingshan Zhong, and Laura Waller, "Computational illumination for high-speed in vitro fourier ptychographic microscopy," *Optica*, vol. 2, no. 10, pp. 904–911, 2015.

[16] Yixiao Yang, Ran Tao, Kaixuan Wei, and Ying Fu, "Dynamic proximal unrolling network for compressive imaging," *Neurocomputing*, vol. 510, pp. 203–217, 2022.

[17] GJ Williams, HM Quiney, BB Dhal, CQ Tran, Keith A Nugent, AG Peele, D Paterson, and MD De Jonge, "Fresnel coherent diffractive imaging," *Physical review letters*, vol. 97, no. 2, pp. 025506, 2006.

[18] Luis B Almeida, "The fractional fourier transform and time-frequency representations," *IEEE Transactions on signal processing*, vol. 42, no. 11, pp. 3084–3091, 1994.

[19] Di Liu, Chuanbin Ge, Yi Xin, Qin Li, and Ran Tao, "Dispersion correction for optical coherence tomography by the stepped detection algorithm in the fractional fourier domain," *Opt. Express*, vol. 28, no. 5, pp. 5919–5935, Mar 2020.

[20] Haldun M Ozaktas and David Mendlovic, "Fractional fourier optics," *JOSA A*, vol. 12, no. 4, pp. 743–751, 1995.

[21] Zeev Zalevsky, David Mendlovic, and Rainer G Dorsch, "Gerchberg–saxton algorithm applied in the fractional fourier or the fresnel domain," *Optics Letters*, vol. 21, no. 12, pp. 842–844, 1996.

[22] Xinhua Su, Ran Tao, and Yongzhe Li, "Phase retrieval from multiple frft measurements based on nonconvex low-rank minimization," *Signal Processing*, vol. 198, pp. 108601, 2022.

[23] SALEH BEA and MC Teich, "Fundamentals of photonics," *Wiley*, p. 313, 1991.

[24] René Escalante and Marcos Raydan, *Alternating projection methods*, SIAM, 2011.

[25] Singanallur V Venkatakrishnan, Charles A Bouman, and Brendt Wohlberg, "Plug-and-play priors for model based reconstruction," in *2013 IEEE Global Conference on Signal and Information Processing*. IEEE, 2013, pp. 945–948.

[26] Ran Tao, Bing Deng, Yue Wang, et al., "Fractional fourier transform and its applications," *Beijing: Tsinghua University*, pp. 285–96, 2009.

[27] C. Candan, M.A. Kutay, and H.M. Ozaktas, "The discrete fractional fourier transform," *IEEE Transactions on Signal Processing*, vol. 48, no. 5, pp. 1329–1337, 2000.

[28] Xin Yuan, "Generalized alternating projection based total variation minimization for compressive sensing," in *2016 IEEE International Conference on Image Processing (ICIP)*. IEEE, 2016, pp. 2539–2543.

[29] Shuhang Gu, Lei Zhang, Wangmeng Zuo, and Xiangchu Feng, "Weighted nuclear norm minimization with application to image denoising," in *Proceedings of the IEEE conference on computer vision and pattern recognition*, 2014, pp. 2862–2869.

[30] Kostadin Dabov, Alessandro Foi, Vladimir Katkovnik, and Karen Egiazarian, "Image denoising with block-matching and 3d filtering," in *Image Processing: Algorithms and Systems, Neural Networks, and Machine Learning*. International Society for Optics and Photonics, 2006, vol. 6064, p. 606414.

[31] Kai Zhang, Wangmeng Zuo, Yunjin Chen, Deyu Meng, and Lei Zhang, "Beyond a gaussian denoiser: Residual learning of deep cnn for image denoising," *IEEE transactions on image processing*, vol. 26, no. 7, pp. 3142–3155, 2017.